ELSEVIER

Catalysis Today 82 (2003) 255–273

CATALYSIS TODAY

www.elsevier.com/locate/cattod

Optimum operation of oxidative coupling of methane in porous ceramic membrane reactors

Y.K. Kao*, L. Lei, Y.S. Lin*

Department of Chemical Engineering, University of Cincinnati, Cincinnati, OH 45221-0171, USA

Abstract

This paper presents analysis of oxidative coupling of methane on Li/MgO packed porous membrane reactor (PMR) by the fixed-bed reactor (FBR) model with reliable reaction kinetic equations. PMR can improve the selectivity and yield by controlling the oxygen feed to the catalyst bed through manipulating the feed pressure. At a fixed methane feed rate there is an optimal oxygen feed pressure that will achieve the highest yield. With a commercial ultrafiltration ceramic membrane, theoretical analysis shows that PMR can achieve, by operating with both side pressures at 1 bar at 750 °C, a maximal 30% yield at 53% selectivity. The maximal yield achieved in the FBR of identical dimension and temperature is 20.7% at 52.5% selectivity. Parametric study shows that lowering the membrane permeability improves the performance. Higher oxygen feed pressure will reduce the yield as well as the selectivity. Homogeneous reactions at high shell-side pressure can have adverse effect on the performance due to the fact that homogeneous reaction rates are strongly pressure dependent. The shell (oxygen feed) side volume must be minimized to reduce the homogeneous reactions. The results of PMR model calculation fit the published experimental result unexpectedly well.

Keywords: Porous membrane reactor; Mathematical model; Optimum operation; Oxidative coupling

1. Introduction

Catalytic oxidative coupling of methane (OCM) represents a large number of partial oxidative reactions with a selectivity problem. Extensive research has been conducted on direct conversion of methane by OCM. However, per-pass C_2 yield on all catalysts reported was limited to about 25% [1]. This is lower than the economically attractive C_2 yield threshold (30%). Membrane reactors have the potential to advance the process industry by enhancing selectivity and yield, reducing energy consumption, improving operation safety, and miniaturizing the reactor system. Over the past decade, several groups studied OCM on catalytically active membrane which changes the OCM reaction mechanism or minimizes the presence of the gas-phase oxygen in the methane stream [2–9]. In these studies, per-pass C_2 yields obtained were around 3–15% though the C_2 selectivity was much higher than that obtained in the co-feed reactors.

A breakthrough in the membrane reactor for OCM was recently reported by Akin and Lin [10]. Based on the results of a theoretical study [11] and membrane material development [8,9], they optimized the conditions for OCM in a dense ionic conducting membrane reactor made of a catalytically active fluorite structured $Bi_{1.5}Y_{0.3}$% $Sm_{0.2}O_3$ (abbreviated as BYS) membrane tube. The BYS is highly oxygen permeable and catalytically active and selective for OCM. Best one-pass C_2 (C_2H_4+C_2H_6) yield achieved for OCM

* Corresponding authors. Tel.: +1-513-55622761; fax: +1-513-5563473.
E-mail address: jlin@alpha.che.uc.edu (Y.K. Kao).

0920-5861/$ – see front matter © 2003 Elsevier B.V. All rights reserved.
doi:10.1016/S0920-5861(03)00240-2

Nomenclature

A	cross-section area of reactor
D	diameter of reactor
$D_{i,\mathrm{K}}$	Knudsen diffusion coefficient of component i
F	molar flow rate
J	permeation flux
P	pressure
q	dimensionless flow rate
$r_{\mathrm{c},1}$	formation rate of carbon dioxide in the catalyst bed
$r_{\mathrm{c},2}$	formation rate of C_2 products in the catalyst bed
$r_{\mathrm{g},1}$	formation rate of carbon dioxide in oxygen feed side
$r_{\mathrm{g},2}$	formation rate of C_2 products in oxygen feed side
y_i	molar fraction of i component
z	reactor length

Superscripts

1	tube (catalyst bed) side
2	shell (oxygen feed) side

Subscript

0	initial condition

in the BYS dead-end membrane reactor was 35% at a C_2 selectivity of 54% at 900 °C. At the same C_2 yield, the membrane reactor mode gives C_2 selectivity of over 200% higher than the co-feed mode in the same membrane reactor under similar conditions.

The membrane reactors described above were all made of dense ionic or mixed-conducting oxide ceramics. During OCM the membrane is subjected to an extremely large oxygen partial gradient (membrane sides exposed, respectively, to oxygen and methane streams). The membrane is inherently unstable due to the chemical expansion induced stress, ion migration and phase segregation. From stability viewpoint, porous ceramic (such as alumina or zirconia) membrane reactor is more attractive for OCM. In fact, three research groups have reported the experimental study of OCM in the membrane reactors made of commercial porous alpha-alumina [12–14] and Vycor glass [15] membranes. The catalyst used by Santamaria and coworkers [12] was Li/MgO and that by the other two groups was Sm_2O_3.

The experimental data reported by the three research groups show that the membrane reactor gives a considerably better selectivity than the fixed-bed reactor (FBR) at low and moderate methane and oxygen conversions. However, the improvement in C_2 yield is marginal. This could be probably because the experiments were not performed under optimal conditions.

The essence of catalyst packed tubular porous ceramic membrane reactor is to control the oxygen concentration for the OCM reaction by feeding oxygen through the membrane wall to optimize the reaction selectivity along the reactor axial direction. This membrane reactor offers potential to increase the C_2 yield. It also allows a more controllable and safer operation for OCM reaction. The operation of a porous membrane reactor (PMR) is in general more complicated than that of a conventional FBR. Theoretical study on the performance of OCM in the porous ceramic membrane is particularly desirable in order to identify the key parameters affecting the reactor performance.

Santamaria et al. [16] performed a simulation study of OCM reaction in a series of packed-bed reactors with oxygen introduced between reactors. Cheng and Shuai [17] reported simulation studies of OCM in plug flow reactors, one with inner wall coated with catalyst and the other a catalyst-coated porous wall with oxygen introduced through the wall. Their work was focused on illustrating the potential improvements on the OCM reaction by controlling the oxygen concentration in the reactor using relatively simple models. In this work, we will present a more systematic simulation study of OCM in porous ceramic membrane reactor packed with catalyst with emphasis on identifying the optimum operating conditions to achieve the highest yield. We will also compare the simulation results with the recently published experimental data on OCM in the PMRs [12,13].

2. Mathematical model

The membrane reactor resembles a tube and shell heat exchanger. Oxygen is fed to the shell side and methane to the tube side of the reactor, which is packed with Li/MgO catalyst. The porous membrane allows all components to permeate through it from both sides.

At a high temperature (>600 °C), gas-phase oxidation reactions also take place in the shell side of the reactor without catalyst. The homogeneous reaction rate has to be significantly lower than the catalytic reaction rates in order for the porous membrane to act like an oxygen semi-permeable dense membrane in distributing oxygen to the catalytic bed. Otherwise, it will act like an FBR with two parallel chambers separated by a non-permselective wall.

2.1. Reaction kinetics

The following OCM reaction kinetic equations derived by Wang and Lin [11] are used to describe the OCM reactions in the Li/MgO catalyst packed tube side of the membrane reactor:

$$r_{c,1} = \frac{K_3 P_{O_2}^{1.251}}{4}\left[\left(1+\frac{8K_2(C_p/C_T)P_{CH_4}}{K_3 P_{O_2}^{1.251}}\right)^{0.5}-1\right] + 16S_0K_2\frac{C_p}{C_T}P_{C_2} \quad (1)$$

$$r_{c,2} = \frac{K_3 P_{O_2}^{1.251}}{16}\left[\left(1+\frac{8K_2(C_p/C_T)P_{CH_4}}{K_3 P_{O_2}^{1.251}}\right)^{0.5}-1\right]^2 - 8S_0K_2\frac{C_p}{C_T}P_{C_2} \quad (2)$$

where C_p and C_T are, respectively, the concentration of electron–hole and total concentration of all defects in the catalyst, determined by the partial pressures of reactants and products as

$$\frac{C_p}{C_T} = \frac{K_1 P_{O_2}^{0.5}}{K_1 P_{O_2}^{0.5} + K_1K_2K_4 + K_2(P_{CH_4} + 8S_0P_{C_2})} \quad (3)$$

and S_0 is the fraction of ethyl radicals that undergo deep oxidation reaction at zero conversion condition:

$$S_0 = \frac{2}{(1+8Z(8K_2P_{CH_4}/K_3P_{O_2}^{1.251}))^{0.5}+1} \quad (4)$$

$$Z = \frac{K_1 P_{O_2}^{0.5}}{K_1 P_{O_2}^{0.5} + K_1K_2K_4 + K_2P_{CH_4}} \quad (5)$$

Values of the rate parameters appearing in the above equations were obtained by linear regression [11] of published experimental data of Tung and Lobban [18], and the results are summarized below:

$$K_1 = 2.472\times10^7\, e^{-49.64(kcal/mol)/RT},$$
$$K_2 = 10.10\, e^{-23.15(kcal/mol)/RT},$$
$$K_3 = 0.103\times10^{-3}\, e^{-4.548(kcal/mol)/RT},$$
$$K_4 = 0.093\times10^{-4}\, e^{27.94(kcal/mol)/RT} \quad (6)$$

The above equations correlate the formation rates (in the unit of mol/cm^3 s) for C_2 and CO_x products to partial pressures (in the unit of atm) of oxygen, methane, and C_2 products, and temperature. Details of the above kinetic model were presented elsewhere [11,19].

It should be pointed out that the above equations were obtained based on the kinetic model which considers oxidation of both methane (methyl radical) the C_2 product (ethylene radical), as detailed in our previous publications [11,20]. The kinetic model was verified by comparing the calculated C_2 yield and selectivity (with the above kinetic equations) with the experimentally data for Li/MgO packed FBRs. The theoretical results agreed very well with the experimental data. For example, with the above kinetic model, the theoretical model for FBR gives the maximum C_2 yield of about 20% in the optimum conditions [20]. This will be discussed in more detail in Section 3.

The following non-catalytic homogenous gas-phase reaction rate equations reported by Lane and Wolf [21] are used to describe gas-phase reaction in the shell side:

$$r_{C_2H_6} = 3.95\times10^5\, e^{-51.8(kcal/mol)/RT}P_{CH_4}^{1.04}P_{O_2}^{1.78},$$
$$r_{C_2H_4} = 9.75\times10^4\, e^{-52.1(kcal/mol)/RT}P_{CH_4}^{1.16}P_{O_2}^{1.62},$$
$$r_{CO} = 3.23\times10^{11}\, e^{-71.6(kcal/mol)/RT}P_{CH_4}^{0.53}P_{O_2}^{3.70},$$
$$r_{CO_2} = 1.02\times10^{-2}\, e^{-29.5(kcal/mol)/RT}P_{CH_4}^{-0.95}P_{O_2}^{1.33},$$
$$r_{CH_4} = 1.10\times10^7\, e^{-54.6(kcal/mol)/RT}P_{CH_4}^{1.04}P_{O_2}^{2.05} \quad (7)$$

At atmospheric pressure, the homogeneous reaction rates are significantly lower than the catalytic reaction rates. For example, at a typical reaction condition: T = 750 °C, P_{CH_4} = 0.7 bar, P_{O_2}=0.3 bar. The catalytic reaction rates of CO_2 and C_2H_6 are one to three orders of magnitude larger than those of the corresponding homogeneous rates.

In general, the oxidative coupling and deep oxidation products are lumped together as two main

products, C_2H_6 and CO_2. We follow the same approach in the following development that the rates are appropriately combined as the following:

$$r_{g,1} = r_{CO} + r_{CO_2}, \qquad r_{g,2} = r_{C_2H_6} + r_{C_2H_4}$$

where r_{CO}, r_{CO_2}, $r_{C_2H_6}$, $r_{C_2H_4}$ are the homogeneous reaction rates as given in Eq. (7).

2.2. Permeation through porous membrane

The gas permeation through the mesoporous membrane (e.g. 4 nm US-Fliter Membranox alumina membrane) involves three mechanisms: Knudsen diffusion, molecular diffusion and viscous flow. At high temperature and low pressure, Knudsen diffusion is the dominant mechanism in the gas permeation. Other mechanisms can be neglected. The support of the commercial mesoporous membrane has a multilayer structure with minimal diffusion resistance. Therefore, the permeation resistance in the support can also be neglected. So in our study, only Knudsen diffusion through the mesoporous top layer is considered and the diffusion flux of each species is calculated according to following equation:

$$J_i = \frac{D_{i,K}}{RT}\frac{(P^1 y_i^1 - P^2 y_i^2)}{\delta}$$

The Knudsen coefficient is calculated by the following formula [22]:

$$D_{i,K} = \frac{2}{3}\frac{\epsilon}{\tau} r \left(\frac{8RT}{\pi M}\right)^{0.5}$$

The membrane parameters are $\epsilon = 0.5$, $\tau = 2.95$, $r = 2 \times 10^{-9}$ m and membrane top-layer thickness $\delta = 5 \times 10^{-5}$ cm for ceramic alumina membrane properties obtained from the literature [23].

The gas-phase reaction may take place inside the pore of the membrane. The homogeneous reactions will affect the permeation flux. Under the anticipated reactor operating conditions ($P_{CH_4} = 1$ bar and $P_{O_2} = 1$ bar), the fluxes of methane and oxygen are 6.267×10^{-5} mol/cm^2 and 4.432×10^{-5} mol/cm^2, respectively. These fluxes are much greater than the gas-phase reactions. Therefore, the amounts of methane and oxygen consumed by OCM reaction inside the pores are very small and its effect on the permeation fluxes can be neglected.

2.3. Reactor model

In the following derivation, superscript 1 stands for inside of the membrane reactor (tube side) packed with catalyst and superscript 2 for outside of the membrane (shell side) and subscript 0 stands for the feed condition. The total pressure of each side of the membrane is constant and the temperatures of the two sides are the same.

Differential mass balances on each species for the tube and the shell side are:

- In the tube side:

$$F_0^1 \frac{d(q^1 y_{CH_4}^1)}{dz} = -A^1(r_{c,1} + 2r_{c,2}) - (\pi D) J_{CH_4} \tag{8}$$

$$F_0^1 \frac{d(q^1 y_{O_2}^1)}{dz} = -A^1(2r_{c,1} + 0.5r_2^1) - (\pi D) J_{O_2} \tag{9}$$

$$F_0^1 \frac{d(q^1 y_{CO_2}^1)}{dz} = A^1 r_{c,1} - (\pi D) J_{CO_2} \tag{10}$$

$$F_0^1 \frac{d(q^1 y_{C_2H_6}^1)}{dz} = A^1 r_{c,2} - (\pi D) J_{C_2H_6} \tag{11}$$

$$F_0^1 \frac{d(q^1 y_{H_2O}^1)}{dz} = A^1(2r_{c,1} + r_{c,2}) - (\pi D) J_{H_2O} \tag{12}$$

It should be noted that the above model assumes uniform radial distribution of the reactant concentrations within the membrane reactor tube. The effect of this assumption on the simulation model can be minimized using the effectiveness factor, as to be discussed later in Section 4.2.

- In the shell side:

$$F_0^2 \frac{d(q^2 y_{CH_4}^2)}{dz} = -A^2(r_{g,1} + 2r_{g,2}) + (\pi D) J_{CH_4} \tag{13}$$

$$F_0^2 \frac{d(q^2 y_{O_2}^2)}{dz} = -A^2(2r_{g,1} + 0.5r_{g,2}) + (\pi D) J_{O_2} \tag{14}$$

$$F_0^2 \frac{d(q^2 y_{CO_2}^2)}{dz} = A^2 r_{g,1} + (\pi D) J_{CO_2} \quad (15)$$

$$F_0^2 \frac{d(q^2 y_{C_2H_6}^2)}{dz} = A^2 r_{g,2} + (\pi D) J_{C_2H_6} \quad (16)$$

$$F_0^2 \frac{d(q^2 y_{H_2O}^2)}{dz} = A^2 (2r_{g,1} + r_{g,2}) + (\pi D) J_{H_2O} \quad (17)$$

Three of the differential balance equations can be replaced by the overall C, H, O atomic number balances:

$$F^1(y_{CH_4}^1 + y_{CO_2}^1 + 2y_{C_2H_6}^1) + F^2(y_{CH_4}^2 + y_{CO_2}^2 + 2y_{C_2H_6}^2) = F_0^1 y_{0,CH_4}^1 \quad (18)$$

$$F^1(2y_{CH_4}^1 + 3y_{C_2H_6}^1 + y_{H_2O}^1) + F^2(2y_{CH_4}^2 + 3y_{C_2H_6}^2 + y_{H_2O}^2) = 2F_0^1 y_{0,CH_4} \quad (19)$$

$$F^1(2y_{O_2}^1 + 2y_{CO_2}^1 + y_{H_2O}^1) + F^2(2y_{O_2}^2 + 2y_{CO_2}^2 + y_{H_2O}^2) = 2F_0^2 y_{0,O_2}^2 \quad (20)$$

In Eqs. (8)–(20), there are total 12 variables $y_{CH_4}^1$, $y_{O_2}^1$, $y_{CO_2}^1$, $y_{C_2H_6}^1$, $y_{H_2O}^1$, q^1, $y_{CH_4}^2$, $y_{O_2}^2$, $y_{CO_2}^2$, $y_{C_2H_6}^2$, $y_{H_2O}^2$, q^2. The above reactor model equations were solved numerically with the Gear's BDF method using the DIVPAG routine of the IMSL® Library (Microsoft).

3. Results and discussion

3.1. Performance of PMR

The dimension of the membrane reactor for the following simulation study is based on a Li/MgO catalyst packed porous tubular ceramic membrane with a inner radius of 0.5 cm. It is surrounded by an outer shell whose dimension provides an effective outer radius of 1 cm. The operating temperature is constant at 750 °C. Table 1 lists the values for parameters used in the following parametric simulation study.

The operation of PMR is limited by the permeation fluxes fixed by transmembrane pressure drop. The amount of oxygen that can be supplied to the catalyst bed, hence the amount of reaction that can take place, will be determined by the pressure on the oxygen feed side. Another operational variation is how the oxygen and methane flow directions are oriented with respect to each other. The flows on the two sides of the reactor can be either co-current or counter-current. Under the counter-current flow configuration, it is very likely that a significant portion of the feed methane will permeate to shell side near the tube-side entrance region because the shell-side methane partial pressure is very low. A large fraction of methane will pass through the shell side without participating in the catalytic reaction and the yield will be low. Therefore, the counter-current flow configuration is not suitable for OCM reaction.

Table 1
List of simulation parameters

Reactor temperature (°C)	750
Reactor length (cm)	10
Tube radius (cm)	0.5
Shell radius (cm)	1
Tube pressure (atm)	1
Shell pressure (atm)	1
Methane permeability (mol/cm^2 bar s)	6.267×10^{-5}
Oxygen permeability (mol/cm^2 bar s)	4.432×10^{-5}

3.2. Concentration profiles

The operating characteristics of PMR can be understood by examining its concentration profiles on both sides of the membrane. The concentration profiles of CH_4, O_2, CO_2 and C_2H_6 on either side of the membrane are shown in Figs. 1 and 2, respectively. Pure methane is fed to the catalyst (tube) side at the rate of 5 cm^3 (STP)/s with pure oxygen to the shell side at a rate of 3.5 cm^3 (STP)/s. The total pressures on both sides are kept at 1 bar.

Fig. 1 shows that the oxygen concentration on the tube side starts at zero and then increases as more oxygen permeates from the shell side and not all of it can be consumed by the oxidative reactions. In the short distance to about 0.5 cm from the inlet, the formation rate of C_2 products by the OCM reactions is greater than the rate of methane undergoes deep oxidation as shown by the greater increase in the C_2 products concentration than that of the carbon dioxide. Oxygen concentration increases and reaches a maximum 16%

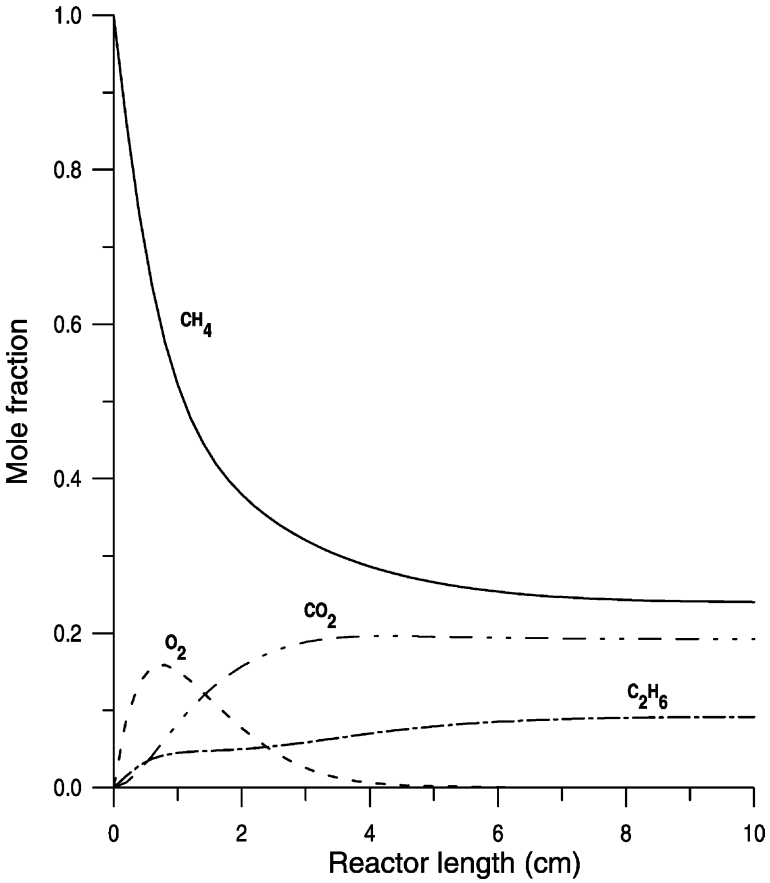

Fig. 1. Concentration profiles on the tube side of PMR.

at about 1 cm from reactor entrance. The maximum occurs as the results of more oxygen is needed for the deep oxidation of not only the feed methane but also the C_2 product produced by OCM reaction. Thus, the carbon dioxide concentration increases more rapidly than the C_2 product concentration. The increasing reaction rates of OCM and, more so, the deep oxidation reactions consume more oxygen than the oxygen supplied through the porous membrane wall. Oxygen concentration decreases. Methane concentration on the tube side decreases rapidly from the entrance due to the reaction and, to a greater degree, to the permeation to the shell side. From the middle of the reactor onward, the oxygen concentration is very low. Low oxygen to methane ratio favors the OCM reaction over deep oxidation reactions. In this region, the C_2 product concentration increases at about the same rate, while the carbon dioxide concentration levels off.

The methane concentration on the shell side as shown in Fig. 2 increases rapidly from the entrance as methane permeates from the tube side. Oxygen concentration decreases rapidly as it permeates to the tube side. The oxidative reaction product also increases along the reactor length. This increase is due mostly to the permeation from the tube side, where catalytic reaction rates are much higher than the corresponding homogeneous reaction rates at the low shell-side total pressure. Near the end of the reactor, partial pressures of all species on both sides become identical.

An overall picture of the reactor performance is represented by the selectivity and yield profiles in Fig. 3. The selectivity drops and the yield increases rapidly

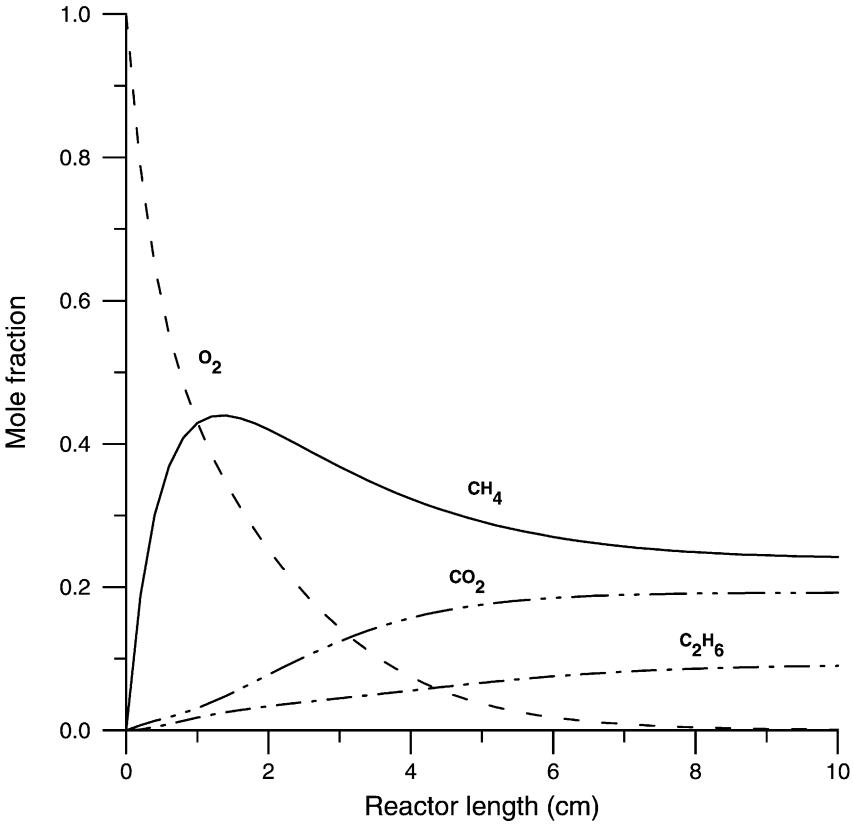

Fig. 2. Concentration profiles on the shell side of PMR.

from the inlet. The rates of both changes are fast due to high oxygen concentration in the catalyst bed. Both OCM and deep oxidation reaction rates increase with oxygen concentration, more so for the deep oxidation reaction. Tube-side oxygen concentration drops to below 3% from 3 cm from the inlet (Fig. 1). The selectivity starts to increase from that point onward. The reverse in the trend of selectivity change is due to the very low oxygen concentration, which favors OCM reaction over the deep oxidation reaction. The operating condition is fairly close to the maximum yield condition. The PMR is able to overcome the FBR's limitation on the maximum yield of 20% in FBR. By distributing oxygen across the membrane, the maximum yield can reach 30%. The selectivity at the maximum yield is about 50%, which is similar to the selectivity at the maximum yield condition of FBR.

The homogeneous reactions taking place on the shell side have only minor effect on the overall performance at low pressures. This effect is more important in the reactor entrance region. In the later part of the reactor, the shell-side oxygen concentration is very low, and the homogeneous reactions have insignificant influence on the performance. This is not true if the shell side is at a higher operating pressure because the homogeneous reactions are strongly dependent on the oxygen partial pressure.

3.3. Yield and selectivity surfaces

The performance of PMR at fixed oxygen and methane feed pressures is determined by both oxygen and methane feed rates. An exhaustive parametric examination of PMR performance is done on a 10 cm long reactor operating at constant feed pressure of 1 bar on both sides. Results are presented in two surface plots, Figs. 4 and 5, that depict the variation in C_2 yield and selectivity as functions of oxygen and

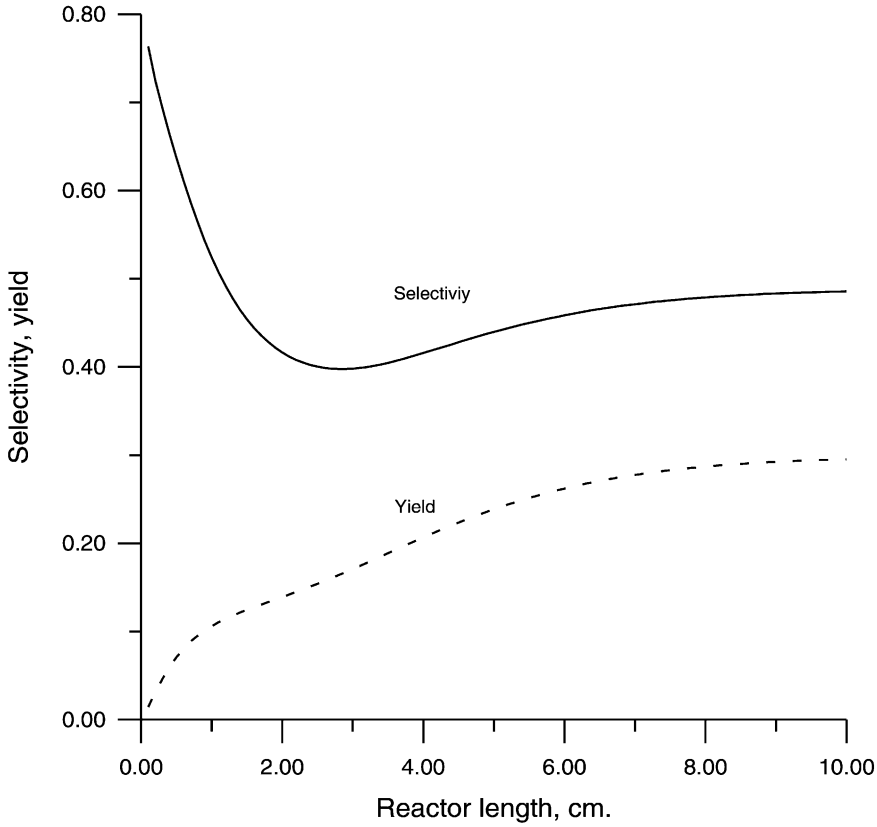

Fig. 3. Selectivity and yield profiles of PMR.

methane feed rates. There is a region of low oxygen feed rates that the 10 cm reactor will be too long with respect to the oxygen supply. For example, at the methane feed rate of 5 cm^3 (STP)/s, the oxygen feed rate has to be greater than 2.5 cm^3 (STP)/s. Below this value, the reactor will be too long.

The selectivity surface plot, Fig. 5, shows that high methane to oxygen feed rate ratio favors the formation of C_2 products. This result is similar to the methane to oxygen feed ratio dependency in FBR: high methane to oxygen ratio favors OCM reaction, thus high selectivity. The highest yield at any methane feed rate occurs at the infeasible region boundary, i.e. by operating the reactor at the lowest feasible oxygen feed rate for any methane feed rate.

The C_2 yield surface as shown in Fig. 5 provides interesting PMR performance characteristics. At a fixed oxygen feed rate, yield initially increases with increasing methane feed rate because high methane to oxygen ratio favors the formation of C_2 products. The yield reaches a maximum and then decrease as the result of a shorter residence time when methane feed rate increases. Similar behavior is also observed as the oxygen feed rate varies at a fixed methane feed rate. Low methane feed rate leads to the oxygen rich reactant mixture that favors the deep oxidation reaction. The C_2 yield increases initially with increasing methane feed rate. The yield will decrease eventually as the residence time decrease when too much methane is fed to the reactor. There is also an optimal oxygen feed rate that maximizes the C_2 yield. For example, at the methane feed rate of 21 cm^3 (STP)/s, the highest yield of 22% is achieved when the oxygen feed rate is about 6 cm^3 (STP)/s (point A in Fig. 4). The selectivity at this highest yield is about 67% (point A in Fig. 5). There is also an optimal methane feed rate

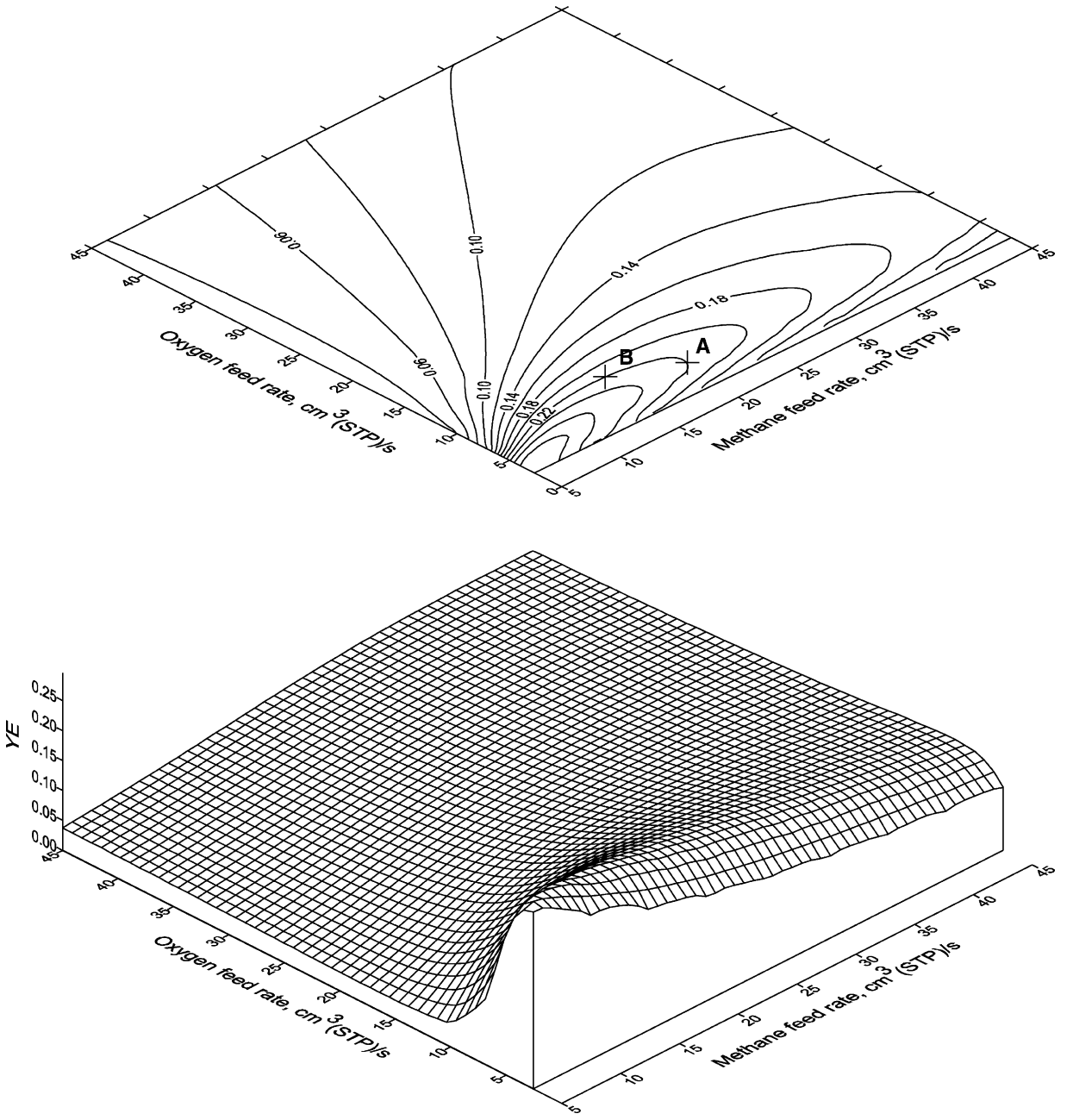

Fig. 4. Yield surface and contour plot of PMR.

at a fixed oxygen feed rate that achieves the highest yield such as point B on the same figures. At an oxygen feed rate of 8.3 cm^3 (STP)/s, the highest yield of 22% is obtained when the methane feed rate is about 15 cm^3 (STP)/s (point B in Fig. 4). The selectivity at this condition is only about 50%. Point A is obviously a better operating condition than point B in the sense that it has a higher selectivity at the same yield. In

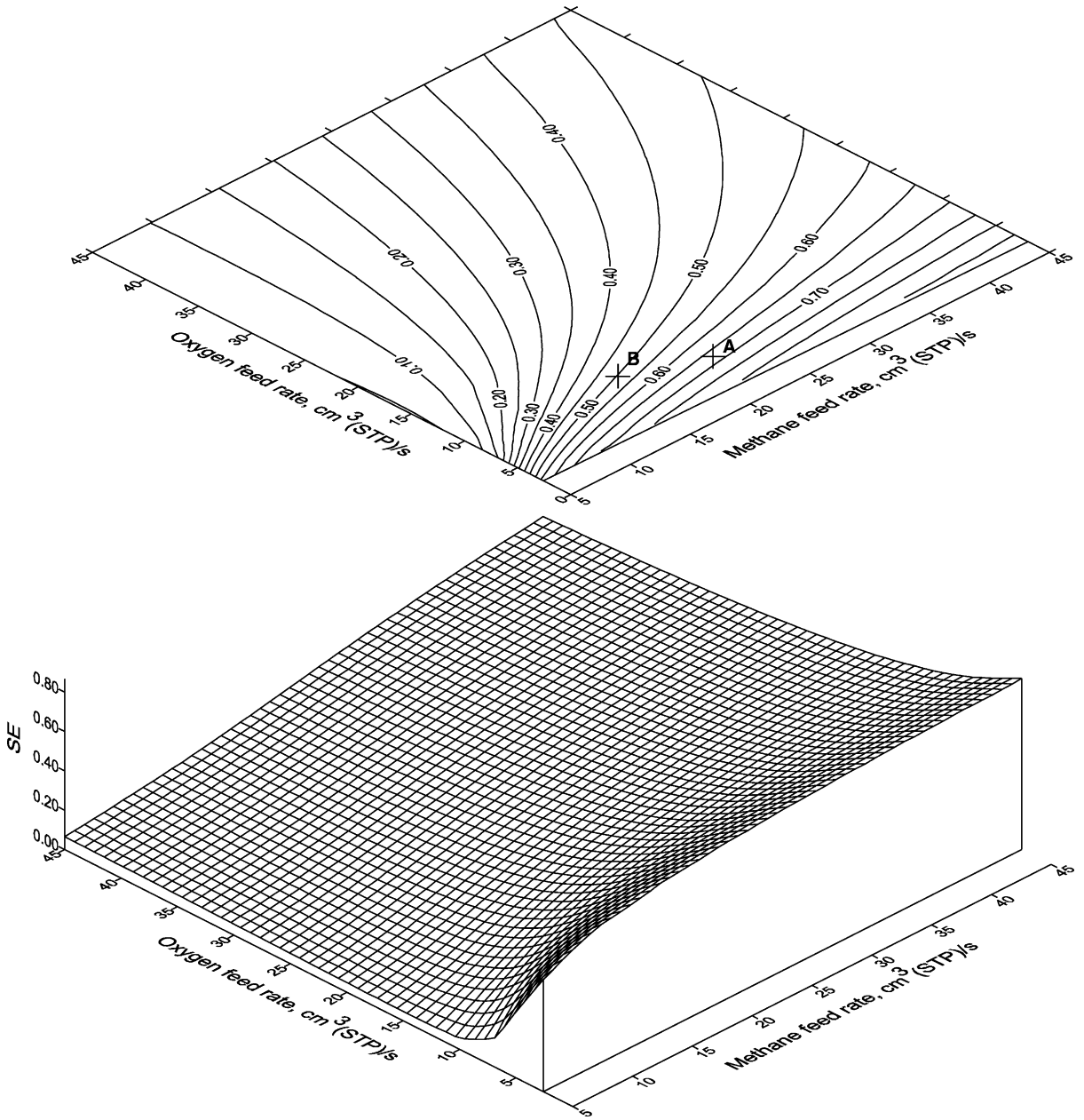

Fig. 5. Selectivity surface and contour plot of PMR.

addition, point A condition also gives higher productivity, since the methane feed rate at point A is higher than that of point B.

The yield surface shows more precipitous changes near the maximum yield in the direction of oxygen feed rate, a less steep change in the direction of methane feed rate. This means that the PMR performance is determined to a greater extent by the oxygen feed rate. The amount of oxygen that can permeate to the catalyst bed in PMR is determined

by the membrane area. When oxygen feed is greater than what can be consumed by the reactions, oxygen concentrations will build up on both sides of the reactor. High oxygen concentration will lead to more deep oxidation reaction. The yield will decrease due to further oxidation of the C_2 products.

There is an optimal operating condition for a reactor with a given membrane area. This condition is located on the lower left corner of the contour plot. For the reactor condition used, the yield is the highest when the oxygen feed rate is 2.6 cm^3 (STP)/s and methane feed rate is 5 cm^3 (STP)/s. The yield is about 30% at the selectivity of 53%.

3.4. Methane and oxygen conversions

The operating characteristics of PMR is rather complex due to the coupling of membrane permeation process with the chemical reactions. The operating characteristics can best be understood by a close scrutiny of the methane and oxygen conversions as a function of their feed rates. The conversions are shown in two contour plots in Fig. 6.

The methane conversion is determined by the oxygen supply and the reactor space–time. Fig. 6(a) shows that the methane conversion as a function of methane and oxygen feed rates. At a constant methane feed rate, the conversion increases rapidly with increasing oxygen feed rate at first as more oxygen is available for reaction. The conversion reaches a maximum at certain oxygen feed rate and then decreases gradually as oxygen feed rate is increased further. This slight decrease is the result of decreasing space–time when more oxygen permeates to the catalyst bed than the reactions can consume. The resulting increase in the total flow rate in the catalyst bed will reduce the reactor space–time. The reduction is more gradual as the permeation flux at a constant pressure differential varies only slightly with concentration. At the lowest methane feed rate examined, the maximal methane conversion is about 75%. The reduction in methane conversion is most pronounced in the low methane feed rate range. In the range of methane feed rate less than 28 cm^3 (STP)/s, there is a certain oxygen feed rate that gives the highest methane conversion.

The oxygen conversion surface (Fig. 6(b)) shows that all oxygen can be consumed at low oxygen feed rates. At a constant oxygen feed rate, the oxygen conversion increases at first with increasing methane feed rate. When the methane feed rate is low, less methane is available for the oxidative reactions. Oxygen consumption increases when more methane is available

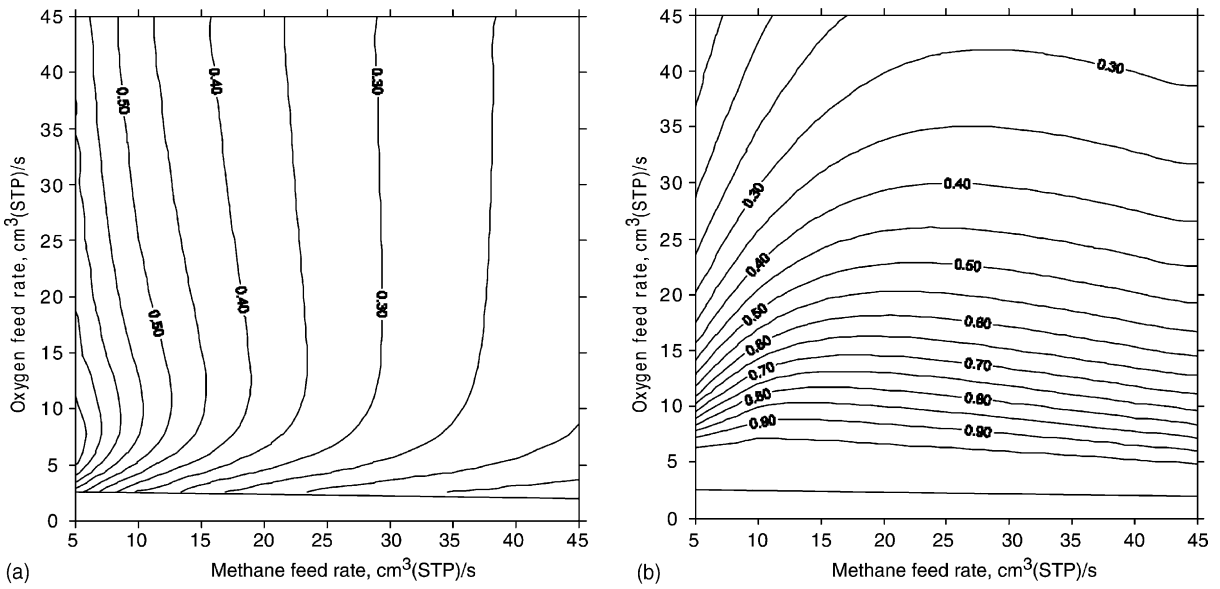

Fig. 6. Methane (a) and oxygen (b) conversion of PMR.

for consuming the oxygen. It reaches a maximum at certain methane feed rate and then decreases as methane feed rate is further increased. Less methane is reacted because of shorter residence time due to the high methane feed rate. Furthermore, the oxygen to methane ratio in the reactor bed at high methane feed rate is very low. This mixture condition favors the OCM reaction which requires 1/4 of oxygen usage of the oxidation reactions. Consequently, less oxygen is consumed and the contour line slope beyond the maximum is flatter.

3.5. *Effect of oxygen feed pressure*

The oxygen permeation flux across the membrane can be controlled by varying the oxygen feed side pressure. Lowering the feed side oxygen pressure reduces the oxygen flux across the membrane, which will reduce the oxygen concentration in the catalyst bed. It is expected that selectivity will improve with decreasing oxygen feed pressure. However, the porous membrane also allows methane to permeate to the oxygen feed side. More methane will leave reactor from the oxygen feed side mostly unreacted except by the homogeneous reactions taking place there. The yield will drop with reducing oxygen feed side pressure. A PMR of the same dimension was used to examine the feed pressure effect. Maximal yields (always obtained at the lowest methane feed rate) at oxygen feed pressure in the range from 0.5 to 1.5 bar is presented in Fig. 7. It shows that the highest yield is achieved with oxygen feed pressure at around 0.8 bar. The selectivity at this pressure is also higher than that at 1 bar feed pressure. Operating the PMR at a higher oxygen feed pressure

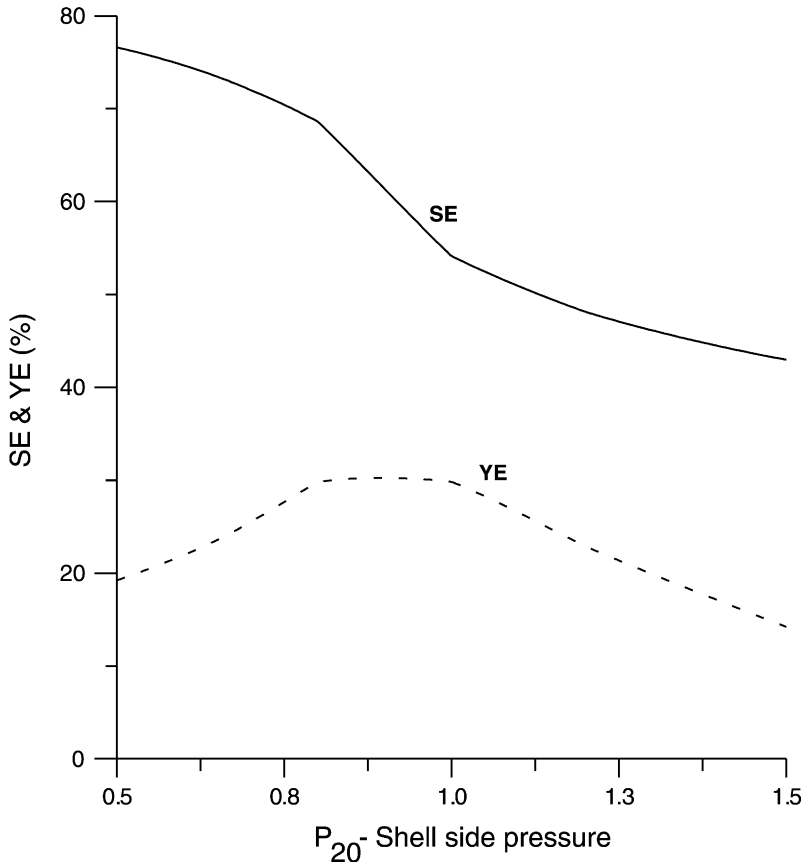

Fig. 7. Maximum yield and the selectivity as a function of oxygen feed pressure.

is definitely undesirable. It causes both selectivity and yield to decrease.

The optimal oxygen feed pressure depends on the membrane permeability. For a membrane with a lower permeability, the highest yield will occur at a higher pressure. The maximal yield is also higher. It should be noted that the homogeneous deep oxidation reaction is strongly dependent on the pressure. The shell-side volume must be kept as low as possible in order to suppress the undesirable homogeneous reactions. It is possible also to prevent the homogeneous reaction from taking place by not allowing the hydrocarbon species to permeate to the oxygen feed side. One of the possibility is to counter the diffusion flux from the reactor tube side to the shell side by maintaining a high hydrodynamic flow from the shell to the tube side. This requires the extension of the present model by replacing the Knudsen diffusion by the dusty-gas model.

3.6. Air as oxygen source

The oxygen feed pressure dependency indicates that low oxygen feed pressure will improve PMR performances. However, low total shell-side pressure allows too much methane to leave the catalyst bed without reaction. The loss of feed methane through the oxygen feed side can be reduced by providing the oxygen feed side with low oxygen partial pressure. An inexpensive source of oxygen is air. The same reactor operating with air as oxygen feed is examined in detail with the methane feed rate ranging from 1 to 45 cm^3 (STP)/s.

The minimal air feed rates at given methane feed rate are higher than using oxygen due to the fact that air contains 21% oxygen. Other than that, the yield surface has similar topography as the surface for pure oxygen feed. On the whole, the yield achieved by an air feed PMR is higher than that achieved by a pure oxygen feed PMR. The contour plot, Fig. 8, shows that

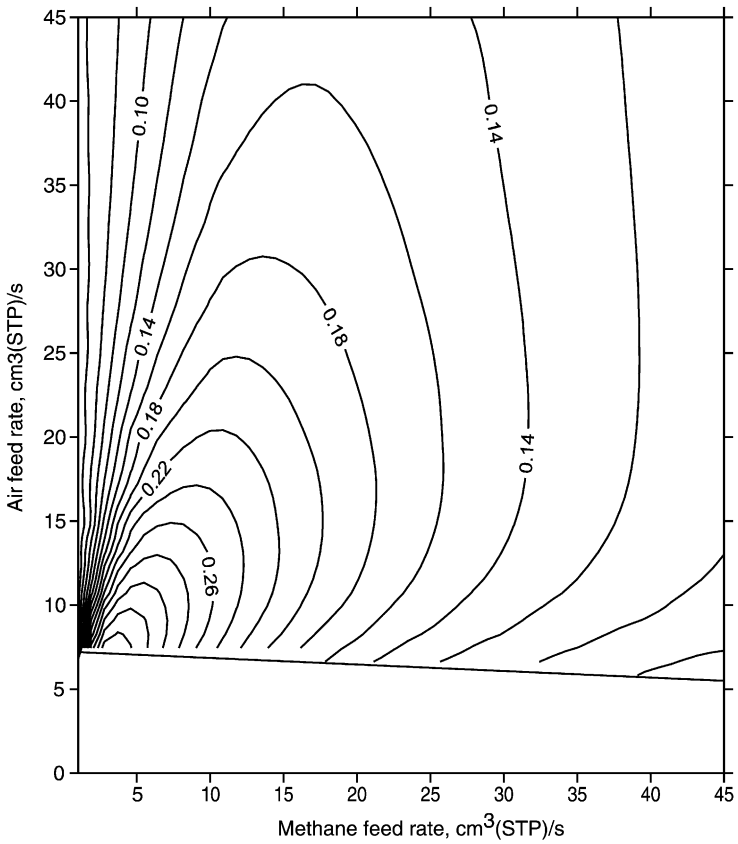

Fig. 8. Contour plot of the yield surface with air as oxygen source.

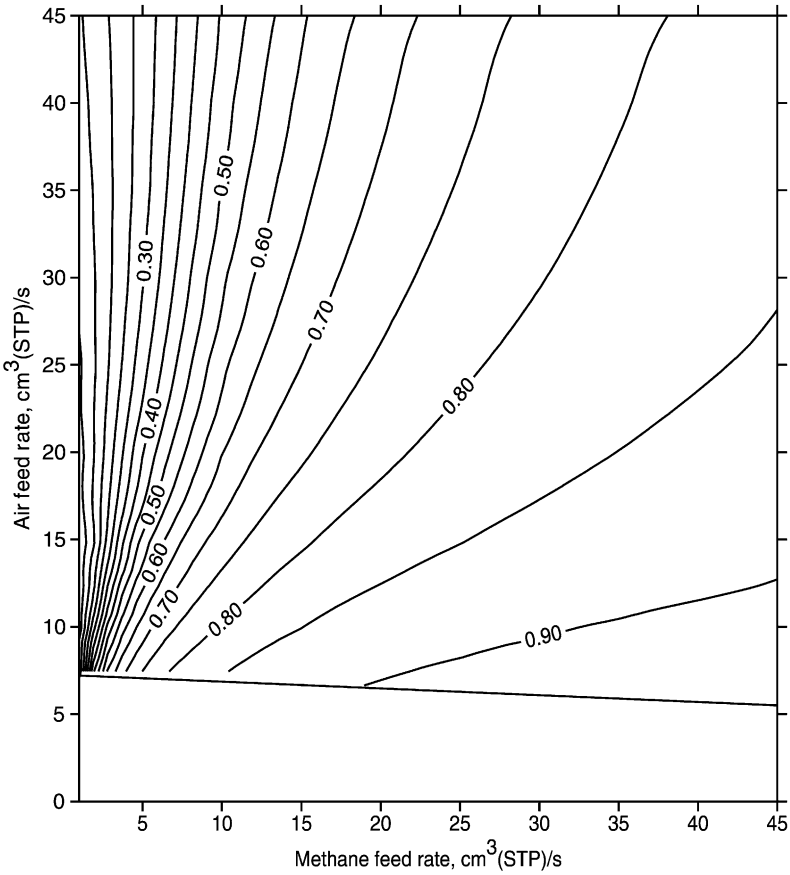

Fig. 9. Contour plot of the selectivity surface with air as oxygen source.

the yield reaches as high as 36% at the optimal feed condition: air feed rate at 7 cm^3 (STP)/s and methane feed rate at 4 cm^3 (STP)/s.

The selectivity surface is also similar to the surface when pure oxygen is used as shell-side feed. The selectivity of a PMR improves when air is used in place of pure oxygen as feed. From the contour plot, Fig. 9, the selectivity at the maximal yield condition is about 70%. This value is higher than the selectivity of 65% at the maximal yield of 30% when pure oxygen is used as the shell-side feed.

3.7. Effect of permeability

The PMR performances can be improved by reducing the oxygen flux across the membrane to the reaction zone. This can be accomplished by modifying the porous membrane to reduce its permeability. Lower oxygen flux will lower the oxygen concentration in the catalyst bed, which can improve the selectivity. When selectivity increases, it will also improve the yield. In the following discussion on the effect of permeability, the porous membrane's permeability is reduced by a factor of 10.

The performance for the case of oxygen feed pressure at 2 bar is shown in Fig. 10 (yield surface contour plot) and Fig. 11 (selectivity contour plot). There is a region of high oxygen feed rate that exceeds the methane feed such that all methane will be consumed in the middle of the reactor. This region was not revealed in the previous plots when the permeability is 10 times larger and the oxygen side pressure is at 1 bar. Otherwise, the topography of both yield and selectivity surfaces is similar to the previous higher permeability

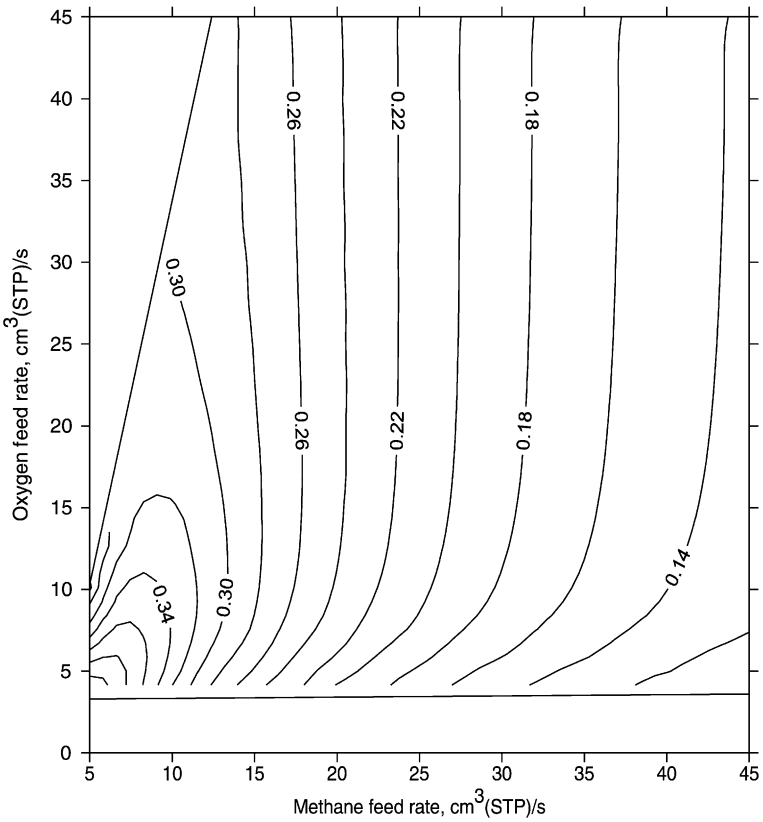

Fig. 10. Contour plot of the yield surface of PMR using membrane with low permeability operating at the oxygen feed pressure of 2 bar.

situation. Lowering the oxygen flux improves the selectivity, which will also increase the yield. The maximal yield is at 43% with the selectivity of 55.2%. The oxygen flux will be smaller when the oxygen side pressure is reduced to 1 bar. The selectivity can reach 69% at the maximal yield of 53%.

4. Comparison study

4.1. Comparison with FBR

A PMR and an FBR with the same physical dimension in terms of catalyst loading and aspect ratio can achieve different maximal yields. The maximal yields, using pure oxygen as the feed, are about 21% for FBR and 30% for PMR. The comparison was made at the maximal yield that an FBR can achieve, which is 20.7%. The best performance for FBR is with a feed mixture consisting 70% methane and 30% oxygen at the mixture feed rate of 25.7 cm^3 (STP)/s. The same maximal yield can be obtained by a PMR of the same dimension at the methane feed rate of 24.5 cm^3 (STP)/s and 6 cm^3 (STP)/s of oxygen to the shell side. The selectivity obtained by the PMR is 69.2% which is considerably higher than that of FBR at 52.3%.

The improvement of PMR is the result of using porous membrane as oxygen distributor. The oxygen concentration in the catalyst bed is lowered throughout the reactor length. Fig. 12 shows the methane and oxygen profiles of PMR and FBR for the cases under comparison. The methane to oxygen composition ratio throughout the PMR is considerably lower than that of the FBR. This favorable mixture composition means more methane can be converted to C_2 products by the OCM reaction instead of deep oxidation reactions, as well as less C_2 products would undergo

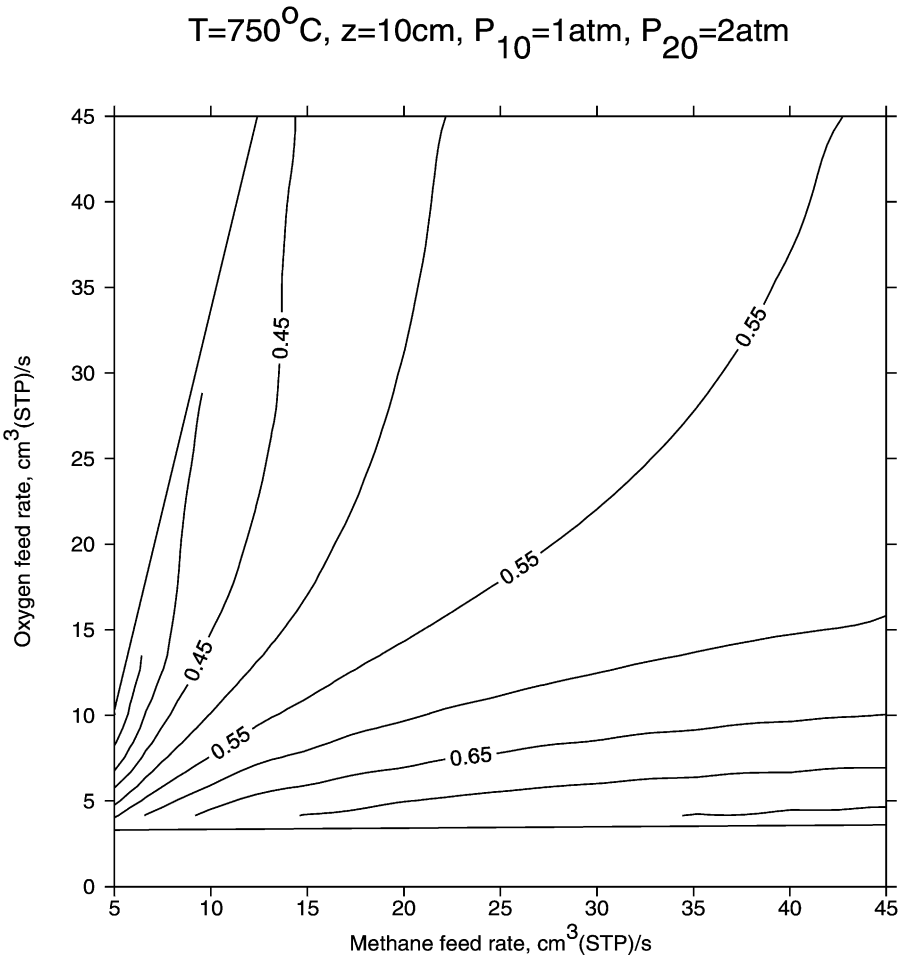

Fig. 11. Contour plot of the selectivity surface of PMR using membrane with low permeability operating at the oxygen feed pressure of 2 bar.

deep oxidation reaction. The selectivity is, therefore, higher.

4.2. Comparison with experimental data

There was only one experimental work [12] reported on OCM in Li/MgO catalyst packed PMR (using a modified alpha-alumina ultrafiltration membrane tube). The original membrane's permeability was reduced by depositing silica inside the membrane pore. The permeabilities reported were about 1/30 of the values used in the above simulation studies. The data reported for the tubular membrane reactor has the exact configuration as the present PMR model. Unfortunately, details of the data conditions were not reported. However, for the cases of the methane to oxygen feed rate of 4:1, there is enough information available that allows a detailed comparison of our model with their data.

The reactor was operated by adjusting the feed side pressure so that the exit flow rate from the oxygen shell side was 5% of the oxygen feed. It is reasonable to assume that the pressure required for a given methane and oxygen feed rate combination to achieve the exit shell-side flow rate to be 5% of its inlet is the same with and without the reaction. The operating pressures at the highest and the lowest feed rate combinations are determined to be 2.6 and 1.23 bar, respectively. This allows the interpolation of operating pressures between the limits.

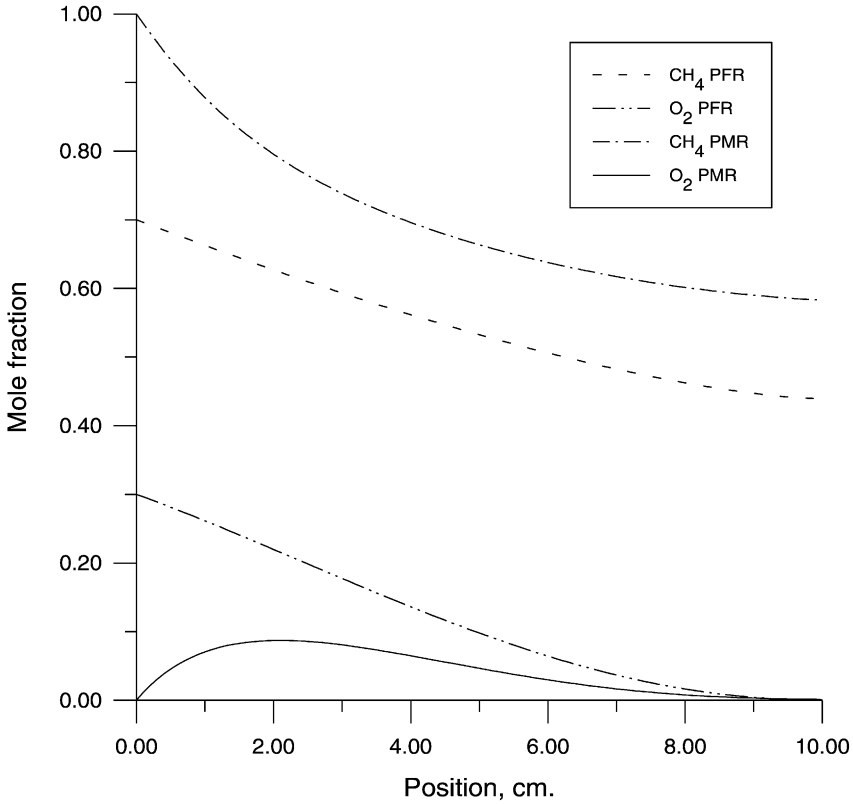

Fig. 12. Comparison of CH_4 and O_2 profile of PMR with FBR.

The actual reactor operation was neither isothermal nor adiabatic. At different flow rates, the temperature profile changes. The average temperature, which was used in the isothermal PMR model, would also change. At the lowest feed rate condition, the reactor would most likely approach the isothermal condition. This condition was used to determine the reaction rates. The catalyst used in their work were Li/MgO catalyst, for which our kinetics (Eqs. (1)–(6)) were developed. However, different preparation methods may result in different activities. In addition, the present reactor model assumes that the mixture composition is uniform in the radial direction. In reality, the concentration varies from the porous wall, where the oxygen partial pressure is the highest, to the lowest at the center of the catalyst bed. A proportional constant was incorporated into the reaction rate expressions of Eqs. (1) and (2) to account for the difference. The best match of the model with the experimental result at the lowest reported feed rate (or largest space–time) is the basis for the determination of the isothermal temperature and the proportional constant. The best fits for isothermal temperature and the proportional constant were determined to be 690 °C and 0.2, respectively.

In the tubular membrane reactor there is a radial oxygen concentration distribution with a maximum near the membrane tube wall. Following the concept of the reaction and diffusion in a porous catalyst cylinder, and reaction rate in the packed-bed within the membrane tube can be correlated to the reactant concentration near the inner membrane tube wall with a correction factor called the effectiveness factor [24]. Eqs. (1) and (2) indicate that the oxygen concentration dependency of the reaction rate is approximated as of first order ($r = kC_{O_2}$). The OCM reaction data provided by Tung and Lobban [18] give the rate constant k of about 7.1 s^{-1} at 600 °C. Assuming that the bed

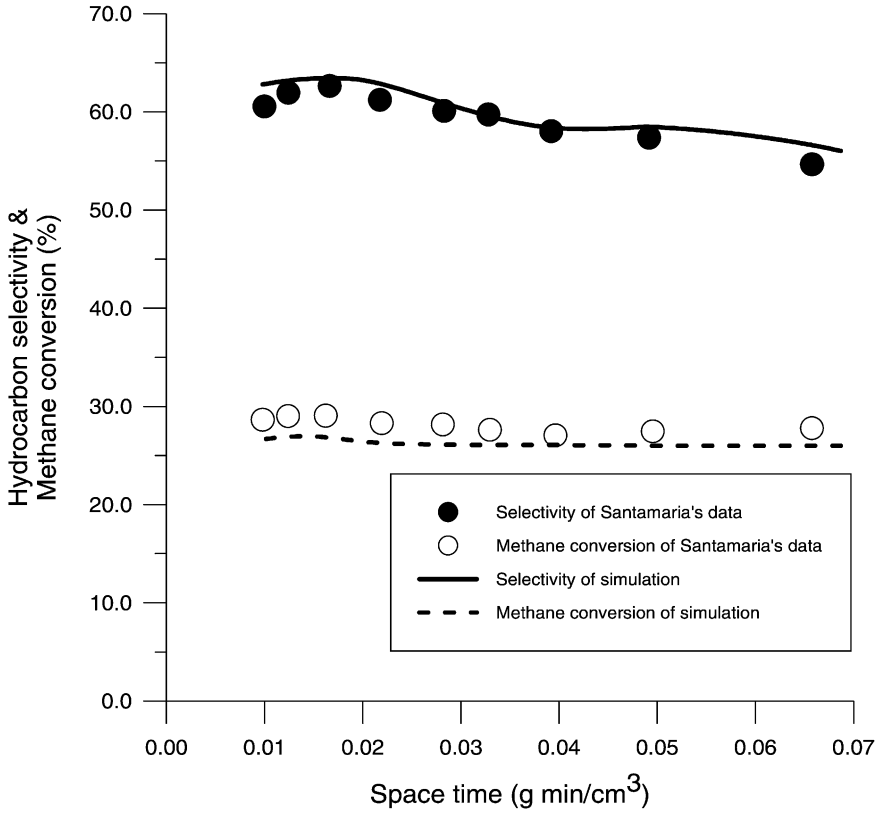

Fig. 13. Comparison of PMR simulation results with experimental data.

porosity of 0.4 and tortuosity factor of 2 for the catalyst packed-bed in the membrane reactor and oxygen diffusion in the catalyst bed is governed by the Knudsen mechanism, the effective oxygen diffusivity in the packed-bed in the membrane tube is estimated at $D_e = 0.12\,cm^2/s$ at 600 °C. With the reactor tube diameter of 1 cm, this gives a Thiele modulus ($=d_{tube}(k/D_e)^{1/2}$) of 8.5, which in turn yields an effectiveness factor of about 0.3 for the cylindrical geometry [24]. This is very close the correction factor of 0.2 used above for comparison of model with the experimental data.

The highest isothermal temperature would be for the case operated at the highest feed rate. This temperature was determined, without changing the proportional constant, to be 790 °C. Since the amount of the reaction heat would be proportional to the feed rates, the isothermal temperature at intermediate flow rates were determined by linear interpolations between these two limits. A number of simulations at intermediate flow rates were generated. The simulation results are plotted with the experimental data in Fig. 13. The model's prediction is remarkably close to the experimental data.

Another model parameter that has influence on the performance is the shell volume. This is especially significant when the shell-side pressure is high because of the strong pressure dependency of the homogeneous reaction rates. In the comparison, the shell-side volume has been kept very small. Otherwise, the shell-side reaction would cause serious degradation in the reactor performance. This point was also stated in the experimental investigation by Santamaria and coworkers [12]. In addition, when the shell-side volume is large, the strongly pressure dependent homogeneous reaction rates also make the computation very stiff. In this case, a solution cannot be obtained.

5. Conclusions

The PMR model was used to examine its performance characteristics. The important operating parameters are the oxygen and methane feed rates. The global pictures of PMR performance are presented in the form of yield and selectivity surfaces. The selectivity of OCM product is improved in a PMR by its ability to control the oxygen concentration in the catalyst bed. This is accomplished by controlling the permeation flux of oxygen via manipulating its feed pressure. It was found that at a fixed methane feed rate there is an optimal oxygen feed pressure that will achieve the highest yield.

With a regular ultrafiltration membrane, PMR at the same dimension used in the FBR can achieve, by operating with pressure in both sides at 1 bar at 750 °C, a maximal 30% yield at 53% selectivity. This is better than the FBR of the same size, which can only achieve maximal yield of 20.7% at 52.5% selectivity at the same temperature. Lower oxygen flux will improve the selectivity, thus also the yield. With atmospheric air as the oxygen feed, the maximal yield is improved to 36% at 70% selectivity.

Lowering the membrane permeability also improves the performance. By reducing the permeability by a factor of 10, the maximal yield obtained with 1 bar oxygen feed is 53% at 79% selectivity. Higher oxygen feed pressure will reduce the yield as well as the selectivity. The homogeneous reactions become significant at high shell-side pressure because the homogeneous reaction rates are strongly pressure dependent. The high oxygen concentration on the shell side has detrimental effect on the selectivity and yield.

References

[1] J.H. Lunsford, Catal. Today 63 (2000) 165.
[2] T. Nozaki, O. Yamazaki, K. Omata, Chem. Eng. Sci. 47 (1992) 2945.
[3] T. Nozaki, K. Fujimoto, T. Nozaki, K. Fujimoto, AIChE J. 40 (1994) 870.
[4] J.E. ten Elshof, J.M. Bouwmeester, H. Verweij, Appl. Catal. A 130 (1995) 195.
[5] S.J. Xu, W.J. Thomson, AIChE J. 43 (1997) 2731.
[6] Y. Zeng, Y.S. Lin, S.L. Swartz, J. Membrane Sci. 150 (1998) 87.
[7] Z. Shao, H. Dong, G. Xiong, Y. Cong, W. Yang, J. Membrane Sci. 183 (2001) 181.
[8] Y. Zeng, Y.S. Lin, J. Catal. 182 (1999) 30.
[9] Y. Zeng, Y.S. Lin, AIChE J. 47 (2000) 436.
[10] F.T. Akin, Y.S. Lin, Catal. Lett. 78 (2002) 239.
[11] W. Wang, Y.S. Lin, J. Membrane Sci. 103 (1995) 219.
[12] D. Lafarga, J. Santamaria, M. Menendez, Chem. Eng. Sci. 49 (1994) 2005.
[13] J. Coronas, J. Santamaria, M. Menendez, Chem. Eng. Sci. 49 (1994) 2015.
[14] A.L. Tonkovic, D.M. Jimenez, J.L. Zilka, G.L. Roberts, Chem. Eng. Sci. 51 (1996) 3051.
[15] A.M. Ramachandra, Y. Lu, Y.H. Ma, W.R. Moser, A.G. Dixon, J. Membrane Sci. 116 (1996) 253.
[16] J. Santamaria, M. Menendez, J.A. Pena, J.I. Barahona, Catal. Today 13 (1992) 353.
[17] S. Cheng, X. Shuai, AIChE J. 41 (1995) 1598.
[18] W.Y. Tung, L. Lobban, Ind. Eng. Chem. Res. 31 (1992) 1621.
[19] W. Wang, Analysis of dense ceramic membrane reactors for the oxidative coupling of methane, MS Thesis, University of Cincinnati, 1994.
[20] Y.K. Kao, L. Luo, Y.S. Lin, Ind. Eng. Chem. Res. 36 (1997) 3583.
[21] G.S. Lane, E.E. Wolf, J. Catal. 113 (1988) 114.
[22] A.M. Allawi, D.J. Gunn, AIChE J. 33 (1987) 766.
[23] J.C.S. Wu, P.K.T. Liu, Ind. Eng. Chem. Res. 31 (1992) 322.
[24] J. Butt, Reaction Kinetics and Reactor Design, Prentice-Hall, New Jersey, 1980, p. 360.